



LC/MS-based non-targeted metabolomics for the investigation of general toxicity of 2,3,7,8-tetrachlorodibenzo-*p*-dioxin in C57BL/6J and DBA/2J mice

Shuhai Lin^a, Zhu Yang^b, Yang Shen^{a,b}, Zongwei Cai^{a,*}

^a Department of Chemistry, Hong Kong Baptist University, Hong Kong, China

^b Department of Physics, Hong Kong Baptist University, Hong Kong, China

ARTICLE INFO

Article history:

Received 4 April 2010

Received in revised form 1 June 2010

Accepted 14 June 2010

Available online 20 June 2010

Keywords:

LC/MS

Metabolomic

TCDD

Toxicity

Differentiating metabolite

ABSTRACT

Although numerous studies have been performed for the toxicological mechanisms of 2,3,7,8-tetrachlorodibenzo-*p*-dioxin (TCDD), the metabolic changes of TCDD toxicity is less well understood. In this study, liquid chromatography/quadrupole time-of-flight mass spectrometry (LC/QTOFMS) was used for non-targeted metabolomics for understanding the different metabolic patterns associated with TCDD exposure in aryl hydrocarbon receptor (AhR) sensitive C57BL/6J (C6) and less sensitive DBA/2J (D2) mouse strains. The serum samples were analyzed and treated with metabolomic analysis in conjunction with multivariate data analysis. Metabolite identification was performed with interpreting high resolution MS data and MS/MS fragmentation, searching against databases and comparing with authentic compounds. Twelve differentiating metabolites (defined as a ≥ 1.5 -fold change with a $P \leq 0.001$) were highlighted in C6 mice versus control group, revealing lipid accumulation, fatty acid beta-oxidation, inflammation and alteration of amino acids as well as phase II drug-like metabolism. In contrast, only 2 differentiating metabolites were detected in D2 mouse model.

© 2010 Elsevier B.V. All rights reserved.

1. Introduction

Mass spectrometry (MS) is a versatile tool in life sciences over the past years. In particular, the emerging field of systems biology, such as genomics, transcriptomics, proteomics and metabolomics, requires dramatic technology advances in analytical sciences [1]. Mass spectrometers when coupled with soft ionization sources play a crucial role in qualitative and quantitative analyses, including the interpretation of post-translational modification and metabolic pathways in biological samples. Atmospheric pressure ionization including electrospray ionization (ESI) has been widely applied in liquid chromatography/mass spectrometry (LC/MS), having rapidly emerged as a popular and powerful tool in metabolomics research. LC/MS not only exhibits good sensitivity, good selectivity and high dynamic range, but also provides soft ionization conditions for intact molecules and metabolic compounds from complex biological matrices. Furthermore, the development of high resolution mass analyzer such as quadrupole time-of-flight mass spectrometry (QTOFMS) covers the identification process from measurement of accurate molecular mass to the confirmation of structural hypothesis [2]. In general, targeted metabolomic approaches are designed for the determination of metabolites in different tested groups with

the comparison to authentic compounds. Non-targeted analyses are performed to uncover general information for the discovery of the known/unknown differentiating metabolites [3]. In non-targeted metabolomic analysis, metabolite identification involves the integrated analysis of accurate mass measurements, MS/MS fragmentation patterns and searching against databases to produce candidate structures that ultimately requires experimental verification [4]. Thus, QTOFMS could be utilized to tentatively identify metabolites belonging to various chemical classes [5]. As the large-scale analysis, the alignment of all extracted mass peaks cross all samples and integration of hundreds even thousands of mass signals are dedicated by softwares, e.g., XCMS [6], MetAlign [7] or MZmine [8]. It is expected that non-targeted approach might be applied to find specific biomarker. For instance, a comparatively overabundant ion was identified to be cholesterol precursor in hepatitis B viral infection and 3-hydroxyhippuric acid in diabetes [9,10]. Some differentiating metabolites, however, could be hardly identified, even using ultrahigh resolution MS analysis [11,12]. In terms of bioinformatics, the classification and data mining such as principal components analysis (PCA), support vector machines [13] and genetic algorithms [14] play a pivotal role. Like other functional genomics technologies, bioinformatics in the emerging metabolomics has been suggested as being the promising tool that could provide an important navigational aid to guide the studies of global intracellular and extracellular metabolites and to produce high dimensional data sets for genome and gene functions [15–17].

* Corresponding author. Tel.: +852 3411 7070; fax: +852 3411 7348.

E-mail address: zwcai@hkbu.edu.hk (Z. Cai).

Polychlorinated aryl hydrocarbons such as dioxins, exemplified by 2,3,7,8-tetrachlorodibenzo-*p*-dioxin (TCDD), belong to the category of highly toxic and persistent organic pollutants that accumulate in animal fat and tissues. The food chain is the main source of dioxins exposure in the human population [18]. Dioxins could cause a broad spectrum of toxic responses in experimental animals and humans including neurotoxicity, liver damage, insulin resistance, immunotoxicity, reproductive toxicity, carcinogenicity and wasting syndromes [18–20]. However, little is known about the metabolic circuits of TCDD toxicity in rodent. Therefore, we examined the toxic effects of TCDD in aryl hydrocarbon receptor (AhR) sensitive C57BL/6J (C6) and less-sensitive strain-DBA/2J (D2) mice [21]. By applying metabolomic approach, several differentiating metabolites were identified within the same LC/MS run with the comparison to the fragment patterns in the databases. Different metabolic patterns in the two mouse strains exposed with the same dosage of TCDD were depicted to elucidate the possible metabolic mechanisms. It is important to note that metabolomics can track endogenous as well as exogenous (xenobiotic) metabolites. Because the metabolism of TCDD by microorganisms appears to be very slow and only two xenobiotic metabolites were identified in the biological samples from Victor Yushchenko [22], the differentiating metabolites could be mostly thought as endogenous biomolecules.

2. Materials and methods

2.1. Chemicals

TCDD (purity >99%) was purchased from AccuStandard, Inc. (New Haven, CT, USA). A stock solution of 4 µg/mL was prepared by dissolving TCDD in corn oil and stored at –20 °C until use. HPLC grade acetonitrile was obtained from Tedia (Fairfield, OH, USA). Pure water was prepared from a Milli-Q Ultrapure water system (Millipore, Billerica, MA, USA).

2.2. Animal experiment and blood sample preparation

Each mouse strain was divided into TCDD dosage and vehicle groups. The C6 mouse experiments involved TCDD group ($n = 7$) and vehicle ($n = 8$), while the D2 mouse numbers were 7 in TCDD group and 5 in vehicle group. The mice were orally administrated with either TCDD at 20 µg/kg d^{–1} in 5 mL corn oil or 5 mL corn oil/kg d^{–1} for consecutive three days. The mice were sacrificed on the seventh day after the first dosing. The mouse blood samples were collected and sera were harvested and stored at –80 °C prior to analysis. After being thawed, 100 µL acetonitrile was added to 50 µL serum sample and vortex vigorously for protein precipitation. The sample was then centrifuged at 13,000 rpm for 10 min at 4 °C. The supernatant was collected and stored in –20 °C until the LC/MS analysis.

2.3. LC/MS and LC/MS/MS analyses

To reduce error associated with instrumental condition variation, samples were run in an order that alternated between the control and TCDD-exposed group. Each sample was analyzed in duplicate. After data integration, the duplicate runs were averaged. Chromatographic separation was performed on an HP1100 HPLC system (Agilent Technologies, Palo Alto, CA, USA) equipped with a 100 mm × 2.1 mm XTerra MS C8 reversed-phase column with particle size 3.5 µm (Waters, Milford, MA, USA). Aliquots of 8 µL each sample were injected onto the HPLC column for analysis. The same linear gradient at a flow rate of 200 µL min^{–1} was used in positive and negative ion mode. The mobile phases consisted of A (0.1% formic acid in water) and B (0.1% formic acid in acetonitrile) for the analysis in positive ion mode, or A (0.1% formic acid and

5 mM ammonium acetate in water) and B (0.1% formic acid and 5 mM ammonium acetate in acetonitrile) for the analysis in negative ion mode. The solvent gradient program started with 5% B, held for 5 min, increased to 90% B from 5 to 13 min, increased to 98% B to 23 min, held for 5 min, then decreased to 5% B in 1 min and re-conditioned for 10 min.

A QTOF mass spectrometer (API Q-STAR Pulsar i, MDS Sciex, Toronto, Canada) was employed for the analysis of metabolite ions. Turbolonspray parameters for ESI-MS were optimized in positive ion mode as follows: ionspray voltage (IS) 5400 V, declustering potential I (DPI) 60 V, declustering potential II (DPII) 15 V and focusing potential (FP) 120 V. The mass range was from 50 to 1000 *m/z*. The ion source gas I (GSI), gas II (GSII), curtain gas (CUR) and collision gas (CAD) were set at 30, 15, 30 and 3, respectively. The temperature of GSII was set at 350 °C. The parameters in negative ion mode were optimized as follows: IS –4100 V, DPI –50 V, DPII –20 V, FP –205 V, and other parameters were same as positive ion mode. Renin substrate tetradecapeptide and taurocholic acid were used for the calibration of the mass spectrometer in positive and negative ion mode, respectively. Data acquisition and processing were performed based on Analyst QS software (service pack 7).

To get identification information of the metabolites, information-dependent acquisition (IDA) mode was used to acquire the MS/MS spectra of the metabolites in serum samples. Using the IDA in Analyst QS (Applied Biosystems/MDS Sciex), MS/MS analysis at different collision energies (CEs) were performed. For the product ion scans, the resolution of the mass resolving quadrupole (Q1) was set low (4 amu window) and different CEs. The ion peaks with peak intensity exceeding 10 counts in the survey scan triggered MS/MS analyses. Former target ions that had been selected for MS/MS analyses were excluded from MS/MS analyses for 60 s. To perform neutral loss scan, ultra-performance liquid chromatography tandem mass spectrometry (UPLC/MS/MS) was employed. Multi-stage MS in ion trap was also performed with direct infusion for characterizing the unknown compound (the method is described in [supplementary information](#)).

2.4. Multivariate and univariate statistical analysis

The LC/MS chromatographic data in the instrument-specific format (.wiff) were converted into NetCDF files and imported to XCMS program (<http://metlin.scripps.edu/download/>) in R for peak finding, nonlinear retention time alignment and grouping. LC/MS data were processed by using XCMS such that bandwidth was set to 10. PCA was also performed in MATLAB R2008a programming environment (The MathWorks, Inc., USA). The one-way analysis of variance (one-way ANOVA) was utilized to compare the TCDD-exposed samples with those of control group for up- or down-regulated metabolites. The *P* values with Bonferroni correction were obtained by One-Way ANOVA in OriginPro 8 software (OriginLab, Co., MA). Human metabolome database (<http://www.hmdb.ca/>) (briefly HMDB), the metlin metabolite database (<http://metlin.scripps.edu/>), massbank (<http://www.massbank.jp/>) and lipidmaps (<http://www.lipidmaps.org/>) were used for metabolite identification.

3. Results and discussion

The schematic chart for the investigation of general toxicity of TCDD in C57BL/6J and DBA/2J mice is illustrated in Fig. 1. General toxicity of TCDD in C6 and D2 mouse models were investigated by analyzing serum sample sets by using LC/QTOFMS (Fig. 1a). One of the total ion chromatograms (TICs) was inserted. Data analysis was performed post-analysis (Fig. 1b): feature selection based

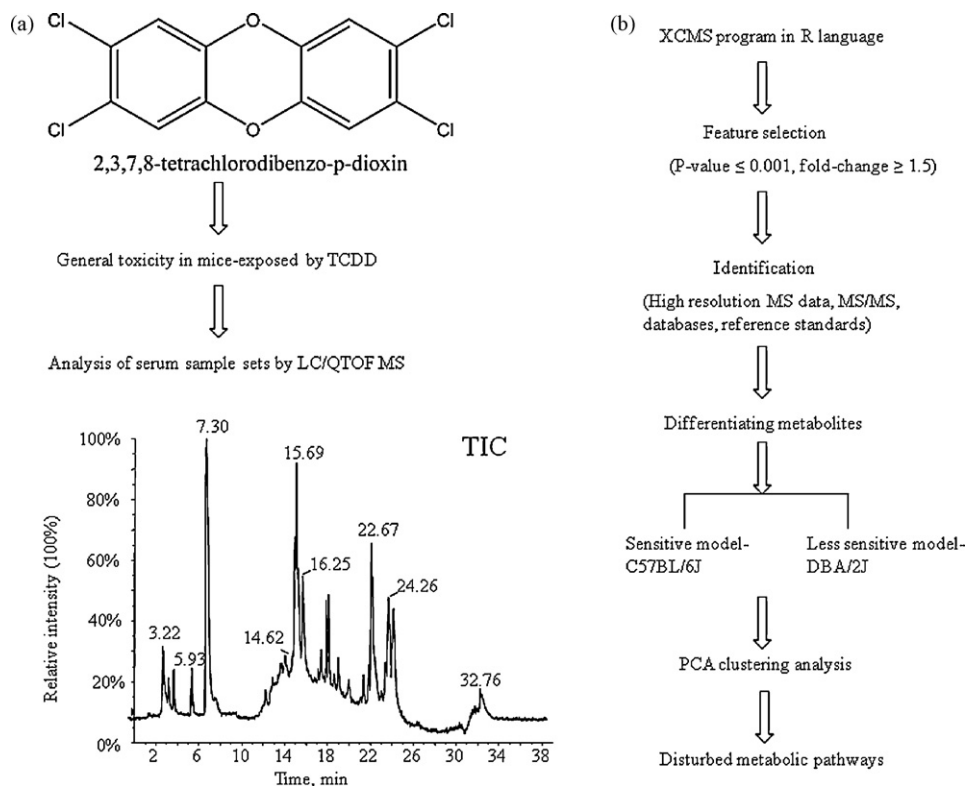


Fig. 1. The schematic flowchart of metabolomics investigation: (a) experimental procedure with the chemical structure of TCDD and one of the typical total ion chromatograms; (b) workflow of data analysis.

on XCMS results from R programming language, then differentiating metabolite identification by high resolution MS data, MS/MS, databases and authentic standards.

3.1. Optimization of LC/MS conditions

Because full scan mode was utilized in non-targeted analysis, LC/MS behavior could be affected by various instrument parameters. Not only modifiers in mobile phase but also ionspray voltage were investigated for investigating the possibility of missing biomarker peaks and the peaks intensity drift. XCMS program in R was performed for the extraction of detected components in different modifiers in mobile phases. The mobile phases consisted of A1 (0.1% formic acid in water), A2 (0.1% formic acid and 5 mM ammonium acetate in water), B1 (0.1% formic acid in acetonitrile) and B2 (0.1% formic acid and 5 mM ammonium acetate in acetonitrile). When A1 and B1 were used in positive ion mode, the resulted data table produced 205 features whereas only 115 features were detected when using A2 and B2. On the other hand, when A2 and B2 were applied in negative ion mode, the data table had 343 features, whereas only 200 components were detected when using A1 and B1. Therefore, the combination of A1 and B1 was utilized in positive ion mode and A2 and B2 in negative ion mode for non-targeted metabolomics. The parameter of high voltage in ion source was also investigated. Three ionspray voltages were investigated in negative (−3500, −3800, and −4100 V) and positive (4600, 5000, and 5400 V) ion mode, respectively.

One sample was injected for six times and the measurement was aligned and visualized by cluster heat map (Figure S1). Higher voltage in the selected ranges yielded higher intensities of most of the extracted ions. Thus, −4100 and 5400 V were adopted for ESI-MS analyses in negative and positive ion mode, respectively.

3.2. LC/QTOFMS revealed different toxic effects of TCDD in two mouse strains

LC/QTOFMS was served as the powerful tool for scanning the metabolites with a diversity of chemical structures. A total of 548 features in C6 and 340 in D2 were observed and integrated in the experiments (Table 1). The selected features ($P \leq 0.01$, fold-change ≥ 1.5) and ($P \leq 0.001$, fold-change ≥ 1.5) represented 37.04% and 20.26% of the total number of features in the data set of C6, respectively; whereas those of D2 accounted for 8.53% and 2.06% of the total number of features in the data set. To obtain the credible differentiating metabolites, we chose the criteria of $P \leq 0.001$ and fold-change ≥ 1.5 as significant differences for feature selection between control and TCDD exposed groups. Interestingly, more proportional discrimination between control and TCDD exposure was observed in C6 compared to D2. In other words, much more metabolites that changed significantly in concentration existed in C6, revealing that C6 was more sensitive to TCDD toxicity than D2. The metabolic phenotyping in mouse blood in less sensitive strain-D2 was disturbed with much less metabolites.

Table 1
Global characterization of the metabolomics data.

Animal model	Total observations	Features ($P \leq 0.01$, fold-change ≥ 1.5)	Features ($P \leq 0.001$, fold-change ≥ 1.5)
C6 mouse model	548	203 (37.04%)	111 (20.26%)
D2 mouse model	340	29 (8.53%)	7 (2.06%)

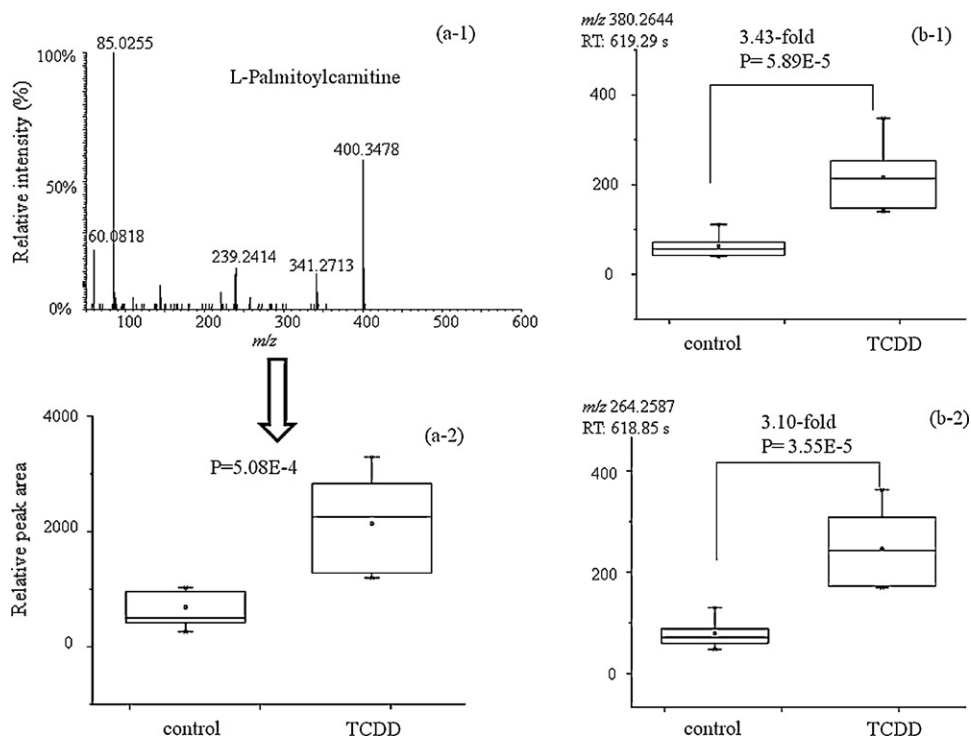


Fig. 2. Identification of L-palmitoylcarnitine by MS/MS analysis (a-1) and box plot of L-palmitoylcarnitine in control versus TCDD group (a-2) as well as box plots of the ion at m/z 380.3244 (RT 619.29 s, b-1) and the ion at m/z 264.3187 (RT 618.85 s, b-2).

3.3. Identification of metabolite candidates

Identification of amino acids and fatty acids by tandem MS fragmentation, retention time and comparison with authentic compounds was a routine approach in non-targeted metabolomic analysis. The acylcarnitine, in particular, could yield characteristic product ions at m/z 60 and m/z 85. L-Palmitoylcarnitine (the ion at m/z 400 in positive ion mode) was detected (Fig. 2a). The MS/MS spectrum of the ion at m/z 426 could not be searched in any database cited here, but HMDB suggests the possibility for three isomers. The ion was tentatively identified to be one of the isomers (elaidic carnitine, oleoylcarnitine or vaccenyl carnitine). Its MS/MS spectrum was shown in Figure S2 as the evidence for proposed structure. It should be noted that the acylcarnitines appeared to be missing when chromatographic mobile phases consisted of ammonium acetate (A2 and B2) in positive ion mode, demonstrating one of the potential problems in non-targeted metabolomics using full scan mode in LC/MS analysis. Interestingly, XCMS table of C6 shown the ion at m/z 380.2644 in the positive ion mode with retention time (RT) 619.29 s significantly increased in TCDD group ($P=5.89E-5$, 3.43-fold change). Another ion at m/z 264.2587 with RT 618.85 s also was up-regulated in TCDD group ($P=3.55E-5$, 3.10-fold change), indicating that the ion at m/z 264 might be the product ion of m/z 380 due to the relatively high ionspray voltage used in the full scan mode of LC/MS (Fig. 2b). This structural hypothesis was confirmed by searching against the Metlin and lipidmaps databases with MS/MS analysis by using IDA method. The metabolite was tentatively identified to be sphingosine-1-phosphate (S1P). The two ions were also observed in the XCMS result of D2 mouse strain, although the relative intensity of the ion at m/z 380 was only increased to 1.57 times in TCDD group versus the control ($P=0.01$).

For lysophosphatidylcholine (LysoPC), its identification has been demonstrated in positive ion mode due to the presence of the characteristic ion at m/z 184 ($C_5H_{14}NO_4P$) in MS/MS analysis [23,24]. Another kind of glycerophospholipid species, namely lysophosphatidylethanolamine (lysoPE), has not been iden-

tified with characteristic ions. Glycerophosphoethanolamine (GPE) species that have the polar headgroup, were diagnosed in negative MS/MS ion mode with fatty acid residues [25]. In our study, the three potential metabolite candidates were significantly changed in C6 mice induced by TCDD. We found that all of them could yield the ions at m/z 196 and m/z 214 in MS/MS spectra, accompanying with neutral loss of 197 Da in negative ion mode (Fig. 3a). On one hand, the ion at m/z 214 was found to match with a candidate in database from high resolution MS data, corresponding to glyceryl phosphorylethanolamine (Fig. 3b-1). On the other hand, another ion at m/z 281 was also observed in the MS/MS spectrum, representing one fatty acid residue ($C_{17}H_{33}COOH$), suggesting the ion at m/z 478.3002 might be a degradative product from GPE. When lysoPE was searched for its chemical structure (Fig. 3a), it could be predicted to produce one fatty acid residue and the polar headgroup ($C_5H_{14}NO_6P$) or its fragment, corresponding to the ion at m/z 214 or m/z 196 in the negative ion mode, respectively. Therefore, the ion at m/z 478.3002 was tentatively identified to be lysoPE (18:1). It should be noted that the ion at m/z 214 could also be considered to be another fragment of 2-aminoethyl 2,3-dihydroxypropyl hydrogen phosphate in the instrumental running according to the chemical structure of lysoPE (Fig. 3b-2). Similarly, the other two ions at m/z 474.2718 and m/z 476.2826 that produced the fatty acids residues with the ions at m/z 277 and m/z 279, respectively, as well as the common neutral loss of 197 Da, were identified to be lysoPE (18:3) and lysoPE (18:2), respectively.

The metabolites were summarized in Tables 2 and 3. It was intractable to identify the compounds which could not be searched against in the current databases or compared with the reference standard available. For instance, depletion of the ion at m/z 339 in negative ion mode was observed in TCDD-exposed group versus control of C6 mice. The peak intensity decreased sharply up to ~200 times due to the toxic effects from extracted ion chromatograms and box plots calculation (Fig. 4a and b). To identify this ion, MS/MS was analyzed in QTOFMS to yield product ion at m/z 163.1947. The neutral loss of 176.0343 was observed, indicating

Identification of LysoPEs in negative ion mode

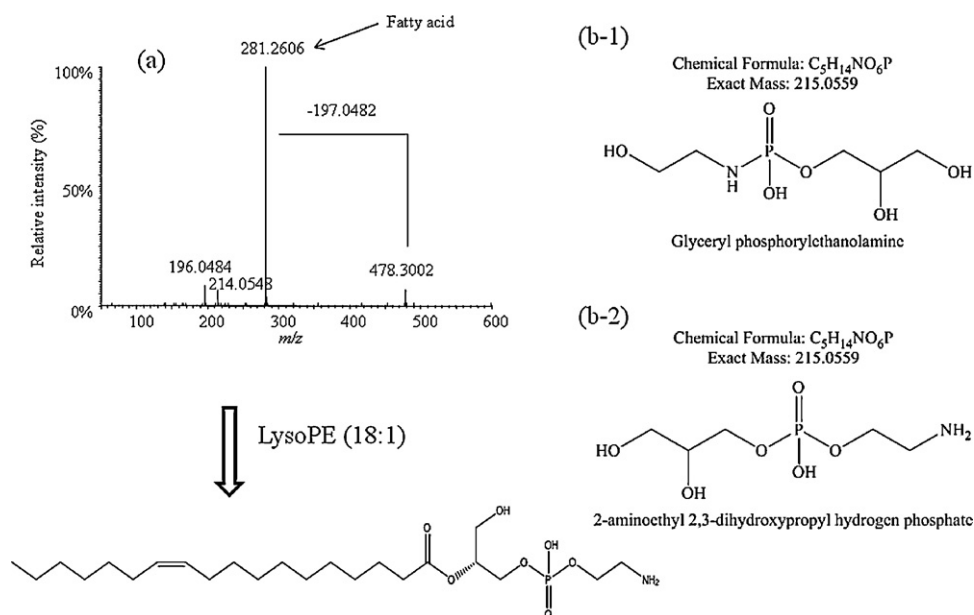


Fig. 3. Identification of lysoPEs in negative ion mode by MS/MS (a) and the possible structure of m/z 215 Da for implicating the structure of LysoPEs (b).

Table 2
Differentiating metabolites in C6 mouse model.

No.	m/z (observed)	Product ions	Differentiating metabolite	Fold-change (P value)	Metabolic pathways
1	474.2718 (–) ^a	277, 196	LysoPE(18:3) ^b	4.54↑ (4.52e–8)	Glycerophospholipid metabolism
2	570.3634 (+)	184, 104	LysoPC(22:5) ^c	4.19↑ (9.89e–7)	
3	476.2826 (–)	279, 196	LysoPE(18:2)	4.50↑ (1.69e–7)	
4	478.3002 (–)	281, 196	LysoPE(18:1)	2.89↑ (7.25e–7)	
5	380.3244 (+)	264	S1P ^d	3.43↑ (5.89e–5)	Sphingolipid metabolism
6	426.3571 (+)	85, 60	Elaidic carnitine /isomers	3.77↑ (4.06e–4)	
7	400.3478 (+)	85, 60	Palmitoylcarnitine	3.11↑ (5.08e–4)	Fatty acid beta-oxidation
8	175.1223 (+)	70	L-Arginine	5.40↓ (7.69e–10)	
9	134.0486 (+)	74	L-Aspartic acid	4.64↓ (8.51e–5)	Amino acid metabolism
10	301.2245 (–)	257	EPA ^e	2.49↓ (6.20e–6)	
11	327.2421 (–)	283	DHA ^f	1.50↓ (5.52e–4)	Biosynthesis of unsaturated fatty acids
12	339.2290 (–)	163	Glucuronide-conjugate	201.68↓ (1.14e–8)	

^a (–): negative ion mode; (+): positive ion mode. ^bLysoPE: lysophosphatidylethanolamine.

^cLysoPC: lysophosphatidylcholine. ^dS1P: sphingosine 1-phosphate. ^eEPA: eicosapentaenoic acid. ^fDHA: docosahexaenoic acid.

that the metabolite candidate was a glucuronide conjugate (Fig. 4c). Glucuronide profiling based on constant neutral loss scan by using UPLC/MS was then applied to confirm the specific glucuronide conjugate (the ion at m/z 339) with markedly reduced concentration caused by TCDD (Fig. 4d). UPLC separation has been demonstrated to be superior to HPLC in non-targeted metabolomic analysis [26]. Multi-stage MSⁿ was further employed to characterize the ion at m/z 339. Product ions at m/z 107 and m/z 147 were observed in MS³ spectrum besides the ion at m/z 163 in MS² spectrum (Fig. 4e). So far, however, this compound could not be exactly identified due to the unavailable standard and corresponding literature report. Notably, a given metabolite usually consisted of several different features including its isotopic cluster and fragment ions. Only the features that were covered in all the samples of at least one group between the two sample sets were involved in the consideration.

As a result, only limited metabolites were listed for differentiating metabolites.

3.4. Multivariate data analysis and metabolic pathway interpretation

The data sets of differentiating metabolites were imported into MATLAB for data visualization. PCA analysis of the profiling data from XCMS showed the separation of two groups in C6 (Fig. 5) and D2 (Fig. 6), respectively. The first two principal components (PCs) accounted for >90% of the variance in the data in either C6 or D2. The number of the differentiating metabolites in D2 was much less than those in sensitive strain. Contribution of each metabolite in PCA model was also visualized. In the case of C6 mouse strain, the TCDD treatment mice could be distinct from control group by using

Table 3
Differentiating metabolites in D2 mouse model.

No.	m/z (observed)	Product ions	Differentiating metabolite	Fold-change (P value)	Metabolic pathways
1	546.3591 (+)	184, 104	LysoPC(20:3)	1.56↑ (2.89e–4)	Glycerophospholipid metabolism
2	580.4428 (+)	184, 104	LysoPC(22:0)	3.65↑ (8.87e–4)	

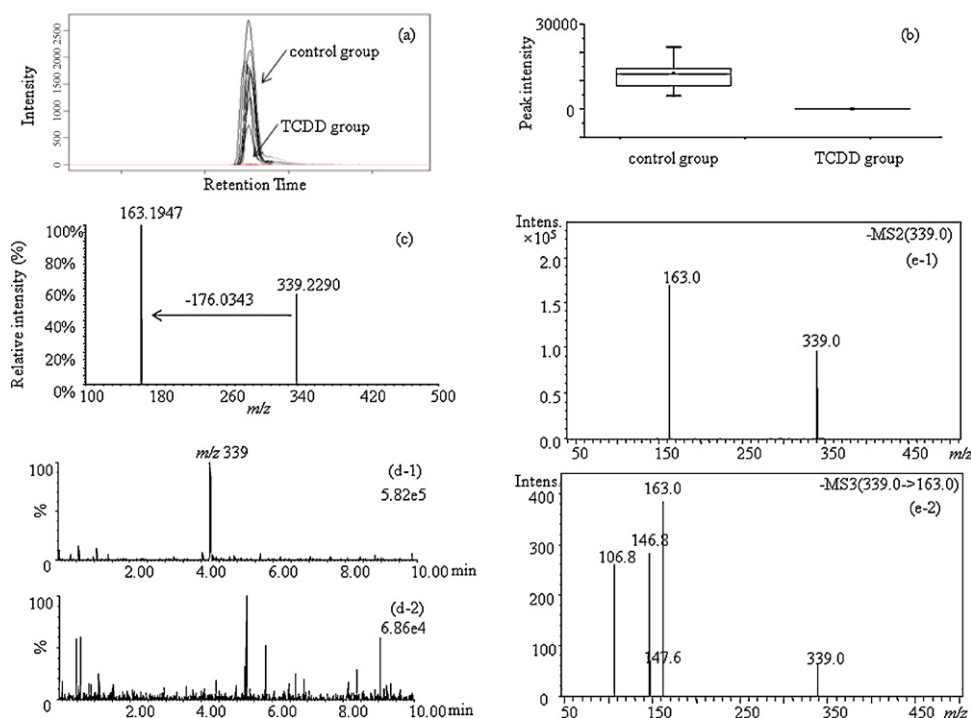


Fig. 4. The unknown metabolite ion was selected as the differentiating metabolite candidate. Extracted ion chromatograms were generated from XCMS program in R (a); box plot was calculated in control and TCDD group (b); neutral loss of 176 Da was observed in MS/MS spectrum of QTOFMS analysis (c). Glucuronide profiling based on constant neutral loss scan was performed by using UPLC/MS/MS: the ion at m/z 339 was extracted from control sample in negative ion mode (d-1); the same ion was not extracted from TCDD sample (d-2). Direct infusion in ITMS was applied for the MS^n analysis of the ion at m/z 339: the ion at m/z 163 in MS^2 (e-1); the ions at m/z 107 and m/z 147 in MS^3 (e-2).

the first principal component (PC1), which accounts 84.86% of the variance only. Concentrations of lysophospholipids, S1P and acylcarnitines were enhanced by TCDD (positive contribution to PC1) while concentrations of amino acids and fatty acids decreased in TCDD treatment mice (negative contribution to PC1) (Fig. 5b-1). And all metabolites had comparable contributions for separation of the two groups. On the other hand, the second principal component (PC2) characterized the individual variations, especially the blood samples among the TCDD treatment group (Fig. 5b-2). S1P, elaidic carnitine and palmitoylcarnitine contributed major part of PC2, which suggested that the response levels of these three metabolites varied in a relatively wider range although they all had significant changes like the other selected metabolites. Thus S1P, elaidic carnitine and palmitoylcarnitine appeared not to be good choices for

hallmarks of TCDD in C6, which may also be associated with the small number of experimental animals. Similarly, the concentrations of the selected metabolites changed very significantly with visualized contributions to PC1 or PC2 for PCA analysis in D2 mouse strain. The TCDD treatment group can be separated from the control group by PC1 only, even if PC1 may catch limited difference between these two groups. The PC2 response was for individuality among the mice, which was consistent with the previous finding that first two PCs (containing most of the variation in the data) would not necessarily capture most of the cluster structure [27].

Regarding the pathophysiological implication of the differentiating metabolites, the lysophospholipid overloading was one of the important hallmarks exposed by TCDD in both of the mouse strains, with the difference that much more lysophospholipids elevated in

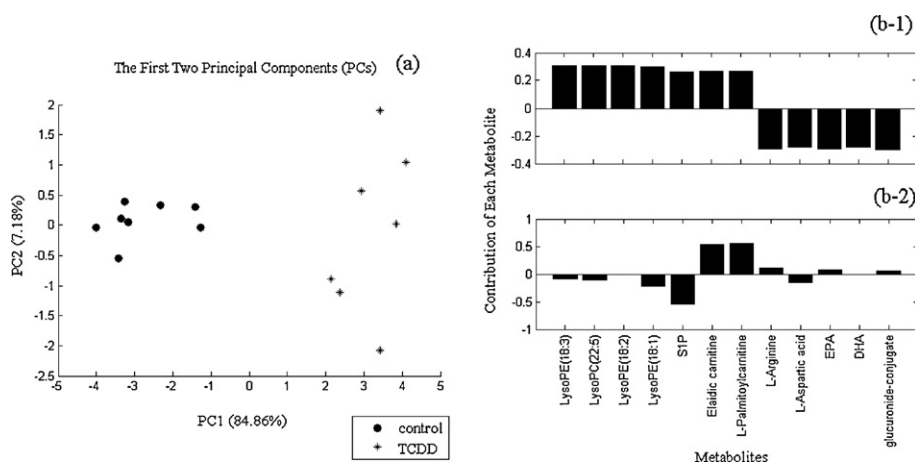


Fig. 5. PCA score plots for C6 mouse model (a) as well as the contribution of each metabolite (column) in PC1 (b-1) and the contribution of each metabolite (column) in PC2 (b-2).

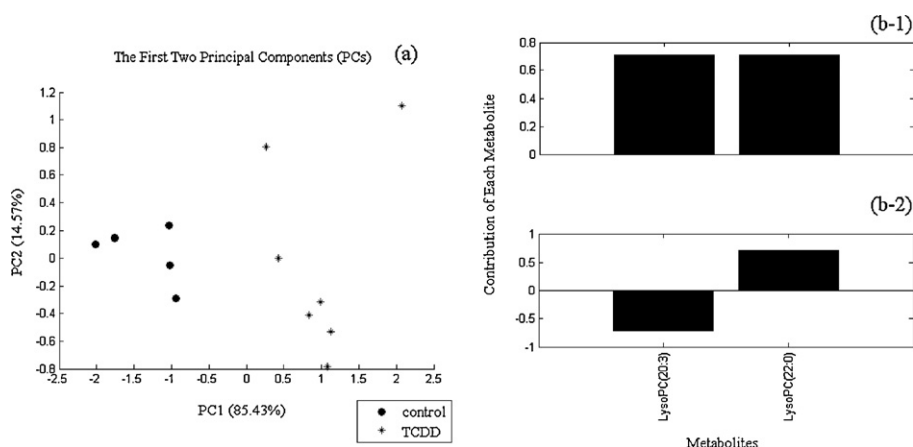


Fig. 6. PCA score plots for D2 mouse model (a) as well as the contribution of each metabolite (column) in PC1 (b-1) and the contribution of each metabolite (column) in PC2 (b-2).

C6 than those in D2. Consistently, TCDD treatment significantly increased the serum triglyceride levels in wild-type, but did not in AhR-knock out mice [28]. Lipid mediator, S1P, is a phosphorylated sphingolipid metabolite with potent bioactive actions in the Sphingolipid metabolism, which controls numerous aspects of cell physiology including cell survival and mammalian inflammatory responses [29]. The compound has also been demonstrated to enhance cyclooxygenase 2 expression and regulate production of eicosanoids (important inflammatory mediators) [30]. The elevated S1P indicated that inflammatory activity may occur in C6-exposed by TCDD versus control. In contrast, TCDD could cause less inflammatory impairment in less-sensitive D2 mice. Reduced eicosapentaenoic acid and docosahexaenoic acid in blood have been linked to inflammation which was consistent with alteration of S1P [31]. Fatty acid beta-oxidation was another notable pathway disturbed by TCDD exposure because acylcarnitine as the transporter for oxidation of fatty acids in the mitochondria increased significantly in C6 mouse strain. However, acylcarnitine did not change significantly in D2 mice [32]. Circulating concentrations of amino acids were markedly decreased in wild type C6 mice, suggesting that impairment of this pathway contributes to the development of the wasting syndrome caused by TCDD.

4. Conclusions

It is well-known that TCDD exhibits its extreme toxicity through AhR binding. Wild type C6 as sensitive mouse strain was used for investigating the toxic effects of TCDD while wild type D2 as less sensitive one was also fed with TCDD as a reference. Our results demonstrated that much less differentiating metabolites in D2 induced by TCDD compared to C6. Lipid overloading, fatty acid beta-oxidation, alteration of amino acids and fatty acids as well as the degradation of a glucuronide-conjugate indicated that a variety of metabolic shifts could be impaired by TCDD in AhR-sensitive mice. LC/MS-based metabolomics as a promising tool revealed that metabolic perturbation was induced by the extremely toxic compound in AhR sensitive mouse as well as less sensitive mouse strain.

Acknowledgements

The authors thank the special post-graduate studentship program of "Persistent Toxic Substances" from Research Grant Council, University Grants Committee of Hong Kong.

Appendix A. Supplementary data

Supplementary data associated with this article can be found, in the online version, at [doi:10.1016/j.ijms.2010.06.012](https://doi.org/10.1016/j.ijms.2010.06.012).

References

- [1] X. Feng, X. Liu, Q. Luo, B.F. Liu, Mass spectrometry in systems biology: an overview, *Mass Spectrom. Rev.* 27 (2008) 635–660.
- [2] E. Werner, J.F. Heilier, C. Ducruix, E. Ezan, C. Junot, J.C. Tabet, Mass spectrometry for the identification of the discriminating signals from metabolomics: current status and future trends, *J. Chromatogr. B: Analyt. Technol. Biomed. Life Sci.* 871 (2008) 143–163.
- [3] V. Shulaev, Metabolomics technology and bioinformatics, *Brief Bioinform.* 7 (2006) 128–139.
- [4] W.R. Wikoff, A.T. Anfora, J. Liu, P.G. Schultz, S.A. Lesley, E.C. Peters, G. Siuzdak, Metabolomics analysis reveals large effects of gut microflora on mammalian blood metabolites, *Proc. Natl. Acad. Sci. U.S.A.* 106 (2009) 3698–3703.
- [5] K. Hanhineva, I. Rogachev, H. Kokko, S. Mintz-Oron, I. Venger, S. Karenlampi, A. Aharoni, Non-targeted analysis of spatial metabolite composition in strawberry (*Fragaria x ananassa*) flowers, *Phytochemistry* 69 (2008) 2463–2481.
- [6] C.A. Smith, E.J. Want, G. O'Maille, R. Abagyan, G. Siuzdak, XCMS: processing mass spectrometry data for metabolite profiling using nonlinear peak alignment, matching, and identification, *Anal. Chem.* 78 (2006) 779–787.
- [7] A. Lommen, MetAlign: interface-driven, versatile metabolomics tool for hyphenated full-scan mass spectrometry data preprocessing, *Anal. Chem.* 81 (2009) 3079–3086.
- [8] M. Katajamaa, J. Miettinen, M. Oresic, MZmine: toolbox for processing and visualization of mass spectrometry based molecular profile data, *Bioinformatics* 22 (2006) 634–636.
- [9] M.A. Rodgers, A. Saghatelian, P.L. Yang, Identification of an overabundant cholesterol precursor in hepatitis B virus replicating cells by untargeted lipid metabolite profiling, *J. Am. Chem. Soc.* 131 (2009) 5030–5031.
- [10] J. Chen, X. Zhao, J. Fritsche, P. Yin, P. Schmitt-Kopplin, W. Wang, X. Lu, H.U. Haring, E.D. Schleicher, R. Lehmann, G. Xu, Practical approach for the identification and isomer elucidation of biomarkers detected in a metabolomic study for the discovery of individuals at risk for diabetes by integrating the chromatographic and mass spectrometric information, *Anal. Chem.* 80 (2008) 1280–1289.
- [11] J. Jansson, B. Willing, M. Lucio, A. Fekete, J. Dickson, J. Halfvarson, C. Tysk, P. Schmitt-Kopplin, Metabolomics reveals metabolic biomarkers of Crohn's disease, *PLoS ONE* 4 (2009) e6386.
- [12] Y. Wang, J. Wang, M. Yao, X. Zhao, J. Fritsche, P. Schmitt-Kopplin, Z. Cai, D. Wan, X. Lu, S. Yang, J. Gu, H.U. Haring, E.D. Schleicher, R. Lehmann, G. Xu, Metabolomics study on the effects of the ginsenoside Rg3 in a beta-cyclodextrin-based formulation on tumor-bearing rats by a fully automatic hydrophilic interaction/reversed-phase column-switching HPLC-ESI-MS approach, *Anal. Chem.* 80 (2008) 4680–4688.
- [13] S. Mahadevan, S.L. Shah, T.J. Marrie, C.M. Slupsky, Analysis of metabolomic data using support vector machines, *Anal. Chem.* 80 (2008) 7562–7570.
- [14] R. Cavill, H.C. Keun, E. Holmes, J.C. Lindon, J.K. Nicholson, T.M. Ebbels, Genetic algorithms for simultaneous variable and sample selection in metabolomics, *Bioinformatics* 25 (2009) 112–118.
- [15] P. Mendes, Emerging bioinformatics for the metabolome, *Brief Bioinform.* 3 (2002) 134–145.
- [16] S.G. Oliver, M.K. Winson, D.B. Kell, F. Baganz, Systematic functional analysis of the yeast genome, *Trends Biotechnol.* 16 (1998) 373–378.
- [17] R.N. Trethewey, Gene discovery via metabolic profiling, *Curr. Opin. Biotechnol.* 12 (2001) 135–138.

- [18] D. Pelclova, P. Urban, J. Preiss, E. Lukas, Z. Fenclova, T. Navratil, Z. Dubska, Z. Senholdova, Adverse health effects in humans exposed to 2,3,7,8-tetrachlorodibenzo-p-dioxin (TCDD), *Rev. Environ. Health* 21 (2006) 119–138.
- [19] J.C. Larsen, Risk assessments of polychlorinated dibenzo-p-dioxins, polychlorinated dibenzofurans, and dioxin-like polychlorinated biphenyls in food, *Mol. Nutr. Food Res.* 50 (2006) 885–896.
- [20] P.A. Kern, S. Said, W.G. Jackson Jr., J.E. Michalek, Insulin sensitivity following agent orange exposure in Vietnam veterans with high blood levels of 2,3,7,8-tetrachlorodibenzo-p-dioxin, *J. Clin. Endocrinol. Metab.* 89 (2004) 4665–4672.
- [21] T. Ishida, S. Kan-o, J. Mutoh, S. Takeda, Y. Ishii, I. Hashiguchi, A. Akamine, H. Yamada, 2,3,7,8-Tetrachlorodibenzo-p-dioxin-induced change in intestinal function and pathology: evidence for the involvement of arylhydrocarbon receptor-mediated alteration of glucose transportation, *Toxicol. Appl. Pharmacol.* 205 (2005) 89–97.
- [22] O. Sorg, M. Zennegg, P. Schmid, R. Fedosyuk, R. Valikhnovskyi, O. Gaide, V. Kniazevych, J.H. Saurat, 2,3,7,8-Tetrachlorodibenzo-p-dioxin (TCDD) poisoning in Victor Yushchenko: identification and measurement of TCDD metabolites, *Lancet* 374 (2009) 1179–1185.
- [23] N. Loftus, K. Miseki, J. Iida, H.G. Gika, G. Theodoridis, I.D. Wilson, Profiling and biomarker identification in plasma from different Zucker rat strains via high mass accuracy multistage mass spectrometric analysis using liquid chromatography/mass spectrometry with a quadrupole ion trap-time of flight mass spectrometer, *Rapid Commun. Mass Spectrom.* 22 (2008) 2547–2554.
- [24] J. Yang, X. Zhao, X. Liu, C. Wang, P. Gao, J. Wang, L. Li, J. Gu, S. Yang, G. Xu, High performance liquid chromatography–mass spectrometry for metabonomics: potential biomarkers for acute deterioration of liver function in chronic hepatitis B, *J. Proteome Res.* 5 (2006) 554–561.
- [25] C. Wang, H. Kong, Y. Guan, J. Yang, J. Gu, S. Yang, G. Xu, Plasma phospholipid metabolic profiling and biomarkers of type 2 diabetes mellitus based on high-performance liquid chromatography/electrospray mass spectrometry and multivariate statistical analysis, *Anal. Chem.* 77 (2005) 4108–4116.
- [26] A. Nordstrom, G. O'Maille, C. Qin, G. Siuzdak, Nonlinear data alignment for UPLC-MS and HPLC-MS based metabolomics: quantitative analysis of endogenous and exogenous metabolites in human serum, *Anal. Chem.* 78 (2006) 3289–3295.
- [27] K.Y. Yeung, W.L. Ruzzo, Principal component analysis for clustering gene expression data, *Bioinformatics* 17 (2001) 763–774.
- [28] K. Minami, M. Nakajima, Y. Fujiki, M. Katoh, F.J. Gonzalez, T. Yokoi, Regulation of insulin-like growth factor binding protein-1 and lipoprotein lipase by the aryl hydrocarbon receptor, *J. Toxicol. Sci.* 33 (2008) 405–413.
- [29] C.E. Chalfant, S. Spiegel, Sphingosine 1-phosphate and ceramide 1-phosphate: expanding roles in cell signaling, *J. Cell Sci.* 118 (2005) 4605–4612.
- [30] M. Dragusin, S. Wehner, S. Kelly, E. Wang, A.H. Merrill Jr., J.C. Kalff, G. van Echten-Deckert, Effects of sphingosine-1-phosphate and ceramide-1-phosphate on rat intestinal smooth muscle cells: implications for postoperative ileus, *FASEB J.* 20 (2006) 1930–1932.
- [31] L. Ferrucci, A. Cherubini, S. Bandinelli, B. Bartali, A. Corsi, F. Lauretani, A. Martin, C. Andres-Lacueva, U. Senin, J.M. Guralnik, Relationship of plasma polyunsaturated fatty acids to circulating inflammatory markers, *J. Clin. Endocrinol. Metab.* 91 (2006) 439–446.
- [32] G. Pierre, A. Macdonald, G. Gray, C. Hendriksz, M.A. Preece, A. Chakrapani, Prospective treatment in carnitine-acylcarnitine translocase deficiency, *J. Inher. Metab. Dis.* 30 (2007) 815.